X-RAY AND EUV CHARACTERISATION OF THE FIRST XMM FLIGHT MODEL MIRROR MODULE

Y. Stockman, E. Mazy, JPh. Tock
Centre Spatial de Liege
Parc industriel du Sart Tilman
4031 Liege
Belgium
phone : 32 4 3676668, fax : 32 4 3675613, email : CSLULG@VM1.ULG.AC.BE.

D. de Chambure, Ph. Gondoin
ESA / ESTEC XMM Project Team
PO BOX 299, 2200 AG Noordwijk, ZH
The Netherlands

ABSTRACT

The first Flight Model Mirror Module with 58 X-ray mirror shells has been tested in the Centre Spatial de Liege (CSL) vertical test facility named FOCAL X. The Flight Model Mirror Module is illuminated by an EUV collimated beam allowing the measurements of the PSF, the effective area, the vignetting and the image quality over the whole field of view. To get a complete characterisation of the mirror module, X-ray measurements are also performed. A pencil beam of 0.5 mm diameter at 1.5 keV and 8 keV allows to measure the reflectivity on selected shells and at several sampled points. This article presents the measurement principles, the analysis undertaken and the deduction of the main characteristics of the XMM first Flight Model Mirror Module.
The impacts of the space qualification tests including thermal and vibration tests on the optical quality of Mirror Module are also exposed.

Keywords : XMM, X-rays telescope, test facility

1. INTRODUCTION

The X-ray Multi Mirror Mission (XMM) satellite has three mirror modules (MM) onboard operating in the 0.1 to 10 keV range. All the MM are made of 58 confocal nested Wolter 1 type mirrors[1]. Each mirror shell (MS) is composed of a parabola of 300 mm and a hyperbola of 300 mm giving an overall length of 600 mm. Their thickness varies from 0.468 to 1.070 mm and their diameter varies between 303.22 to 693.1 mm. A replica technique by nickel electroforming the mirror from an Aluminium mandrel is used. The microroughness of each optical surface is better than 7 Å usually better than 4 Å. The weight of one MM is 425 kg. The specifications for a MM are :

- a Half Energy Width (HEW) of 16.5 arcsec at 58.4 nm
- an effective area of 1475 cm_ at 1.5 keV and 580 cm_ at 8 keV.
- a 7500 mm focal length +/- 5 mm.

The first FM1 was sent to CSL beginning 1997 for optical characterisation and space qualification measurement. A view of the Flight Model 1 (FM1) inside the test facility FOCAL X is presented in figure 1.

Tests performed on FM1 in February and March 97 are briefly reported in this paper. Two types of tests are performed : on one hand environmental tests simulating mechanical and the thermal stresses endured by the MM during it operational life and on the other hand optical tests, checking that the MM optical performance is not alterated after the environmental tests.

The environmental tests consist of thermal cycling and vibration tests around 3 orthogonal axis.

The optical tests are divided in two main steps using different optical set ups : one in the Extreme Ultra Violet (EUV) in full collimated illumination, and the other with a X-ray pencil beam of 0.5 mm diameter at pupil entrance level.

The use of the EUV channel provides the Point Spread Function (PSF) at 58.4 nm and by computation the Encircled Energy Function (EEF) at different focus positions and in the Field Of View (FOV). Analysis on extra focal images for diagnostic purposes and effective area at 58.4 nm measurements are also performed.
The X ray pencil beam channel allows to determine the shells position with respect to each other, and to measure the local reflectivity at 1.5 and 8 keV.

FIGURE 1. FM1 IN FOCALX FACILITY

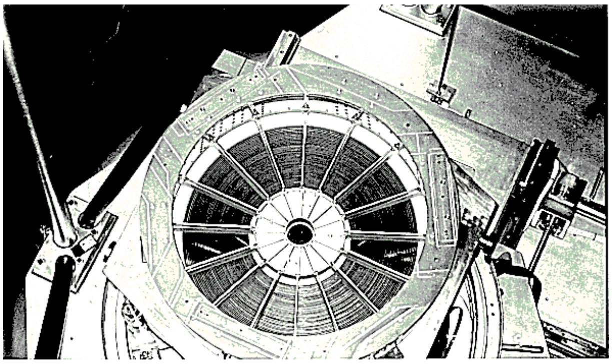

2. TEST PLAN

Beginning of February 97 the first XMM MM FM1 arrived at CSL. Ten days in FOCALX were required to make a first optical characterisation, used as reference for the following optical tests. On the 11th of March the FM1 MM was integrated and instrumented in FOCAL2 facility for thermal cycling. Three thermal cycles ranging from - 15 °C to + 40 °C were applied on the MM. The temperatures applied on the shrouds and the telescope are presented in the plot of figure 2. Care is taken to avoid gradient higher than 5 °C between the spider supporting the MS and the external skin. An other tests sequence of ten days in FOCAL X took place to check that the optical quality of the FM1 MM was not degraded by the thermal cycling tests. On the 13 th of March the FM1 MM was moved to the shaker facility. The applied accelerations are presented in table 1. The achieved values are the ones expected from the mathematical model. A last optical test is then performed. A flow chart of this test sequence is presented in figure 3.

FIGURE 2.A : TEMPERATURE DURING THERMAL CYCLING

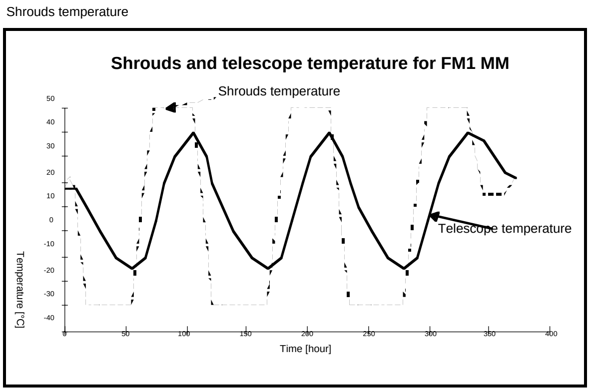

TABLE 1 : VIBRATION TESTS RESULTS

FM1 VIBRATION

	X axis	Y axis	Z axis
Max sine input	**10 g**	**6.7 g**	**6.8 g**
Max sine response	**15.1 g**	**10.4 g**	**10.6 g**
	spider centre	**blocking shell**	**blocking shell**
Max random response	**5.6 g_{rms}**	**4.4 g_{rms}**	**4.7 g_{rms}**
	MSP I/F frame	**blocking shell**	**blocking shell**
Fundamental frequency	**113 Hz**	**55 Hz**	**55 Hz**

FIGURE 3 : TEST FLOW CHART

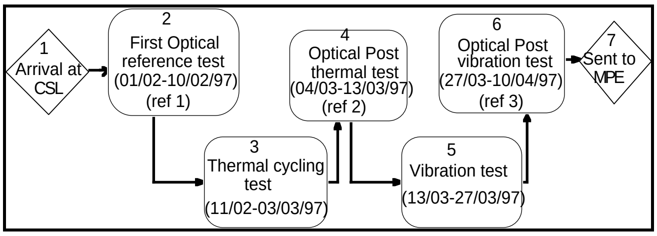

3. EUV MEASUREMENTS

3.1. Introduction

EUV measurements are performed to have a quick assessment of the image quality of the complete MM for a source at infinite distance without being limited by the diffraction effects. The choice of 58.4 nm shows that the diffraction is about 4 arcsec HEW and therefore negligible with respect to an expected HEW of 16 arcsec. The other reason to select this wavelength is the possibility of creating a large collimated beam using classical technology in terms of facility design (Cassegrain collimator design, monolayer coating, commercial sources, CCD detector, ...availability).

3.2. Set-up description

The EUV channel consists of an Electron Cyclotron Resonance source fed with He and providing He I and He II lines. The source is put in front of a 100 µm pinhole located at the focal point of a Cassegrain collimator of 800 mm external diameter and 250 internal obstruction diameter. This system provides a collimated beam with 2 arcsec divergence illuminating completely the MM. The MM focalised the beam on a back side illuminated CCD, through an Al filter to reject all the visible light. A general layout of the EUV channel is presented in figure 4 and more detailed descriptions are available in ref. 2, 3.

FIGURE 4 : EUV CHANNEL GENERAL LAYOUT

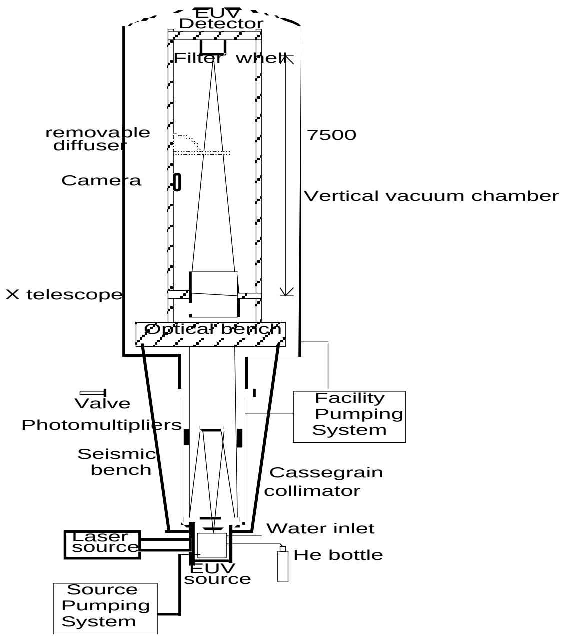

3.3. Measurements

The first measurement consists in recording the light reaching on the CCD detector placed at the nominal focal length of the MM. This provides the PSF at nominal focus. To check the correct alignment with respect to the incoming collimated beam the total energy of extra focal images is measured versus the FOV. The MM is then aligned on the maximum flux and a through focus scan is performed to determine the focal length. At the determined best focus position PSF's are recorded and EEF are computed. For diagnostic purposes several out of focus images are taken in the complete FOV. Finally effective area is measured.

3.4. Results

Figure 5 represents the PSF observed at the nominal focus after thermal test. The central peak is quite narrow (Full Width at Half Maximum (FWHM) is less than 7 arcsec) and is unique. This confirms that all the shells are coaligned. Further analysis will be presented on the best focus PSF.
The alignment under vacuum is performed by optimising the throughput of the MM versus the FOV. The FOV is scanned from - 5 arcmin to + 5 arcmin by step of 0.5 arcmin following two orthogonal azimuths. An example of result is presented in figure 6. The results for the three optical tests show no difference inside the measurement accuracy evaluated to +/- 10 arcsec.

FIGURE 5 : PSF AT THE NOMINAL FOCUS AFTER THERMAL TEST

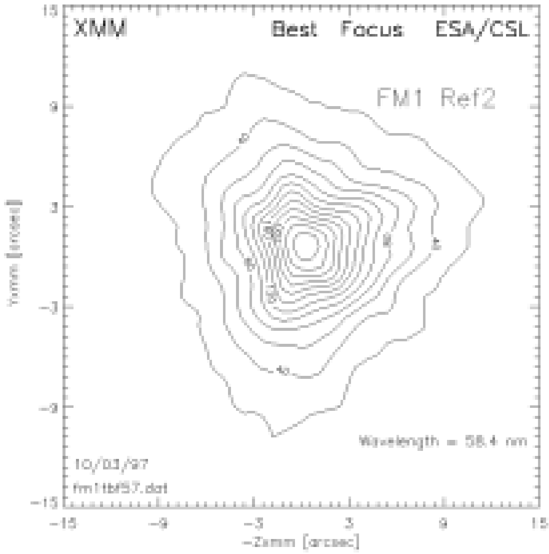

The focal plane is found by stepping along X axis (optical axis) by steps of 2 mm and computing the HEW. An example of HEW versus focus position is plotted in figure 7. It is observed that no variation occurs after the environmental tests. Peak to valley difference is 130 µm. This has no impact on the HEW once the detector is placed at the best focus position since as it can also be observed from these curves that the system presents a large depth of focus. The achieved focal length is 7495.3 mm instead of the 7500 specified.
Plenty of best focus images were taken during these three test campaigns for deeper analysis in order to confirm the final results. The EEF presented in figure 8 of the best focus position are computed on an image achieved by adding 50 images. The achieved values are presented in the table 2. The FM1 MM shows an HEW of 15.5 arcsec after all the environmental tests, that is 1 arcsec better than specified.

TABLE 2 : HEW, 90EW AND FWHM COMPUTED AFTER EACH ENVIRONMENTAL TESTS AT 7495.3 MM

Test campaign [arcsec]	REF	POST_ THER	POST_ VIB
HEW	15.7	15.4	15.5
90EW	61.4	62.4	62.6
FWHM	6.7	7	6.7

Extra focal images give additional information, and they show change after the vibration tests. The two images presented in figures 9.a and 9.b are + 100 mm enhanced extra focal images taken before and after the vibration tests. A loop going outside the annular shape between the 1 and 2 o'clock sector appears. Nowadays it is not clear if it is due to one or several shells and if it is internal stress on the mirror, a stress from the spider to the mirror(s) or a gluing problem. Anyway, this has no observable impact on the best focus image quality. From these extra focal images the azimuthal distribution is computed, and a 1 % RMS variation is observed over the 16 sector intensity.

The final measurement with the EUV beam is the effective area measurement. Applying the next formula

$$Effarea = \frac{I_{Extfoc} \cdot CCDarea}{I_{Flatfield}}$$

where I_{Extfoc} is the intensity of the extrafocal image [Digital Unit/s], CCDarea is the CCD area (4.66 cm_) and $I_{Flatfield}$ the intensity of the incoming flux [Digital Unit/s], gives the values presented in table 3.

TABLE 3. EFFECTIVE AREA MEASURED AFTER EACH ENVIRONMENTAL TESTS

Test campaign Theory = 1817 cm_	REF. 1	REF. 2	REF. 3
Effective area in cm_	1673	1631	1555

Possible explanations have been raised to justify the systematic decrease of effective area. Up to now none of them is fully satisfactory, so that deeper analysis and additional measurements are planned.

FIGURE 6 : BEST TILT ALIGNMENT CURVES

FIGURE 7 : BEST FOCUS CURVES (HEW VS. FOCAL LENGTH)

FIGURE 8 : EEF FOR BEST FOCUS IMAGE

FIGURE 9 A AND B : + 100 MM ENHANCED EXTRA FOCAL IMAGES TAKEN BEFORE (A) AND AFTER (B) THE VIBRATION TESTS.

A

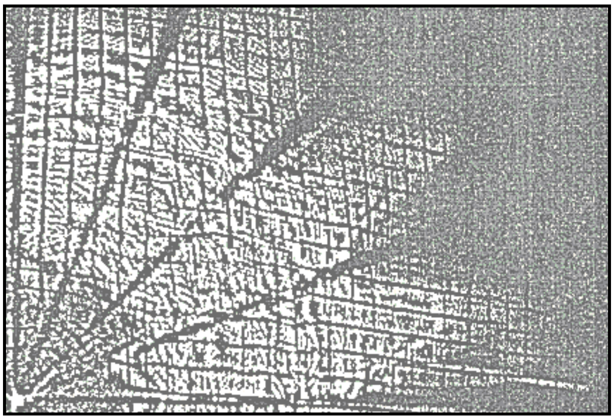

B

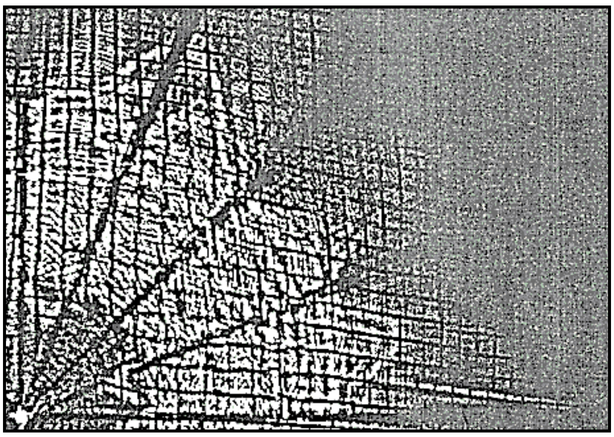

4. X-RAY MEASUREMENTS

4.1. Introduction

The X-ray measurements are required to monitor the reflectivity and to measure the possible contamination evolution due to the environmental tests. To achieve these goals a simple optical system is used as already described in details in ref. 2 and 3 and reminded here in a few words.

4.2. X-ray experimental set-up

A general overview of the experimental set-up is depicted in figure 10. It consists of a source package, 2 pinholes and a detector unit. This system provides a slightly divergent pencil beam with a size smaller than the width of a shell aperture.
The source package consists of a X-ray generator equipped with two kinds of target. A copper target providing 8.04 keV Cu-K emission line and Al target providing 1.49 keV Al-K‾. A filter wheel is placed in front of the source to select the appropriate energy level.
A first pinhole of 0.3 mm diameter is integrated into the source at 35 mm from the anode and a second pinhole of 0.3 mm diameter is located at 7540 mm from this first one. This configuration defines a beam with a 0.5 mm diameter at shell level. The beam is deviated to the telescope focal plane via the shell parabola and hyperbola combination. In this focal plane a solid state detector of 20 mm diameter without spatial resolution collects the photons.
The solid state detector is made of a germanium crystal; it is closed by a mesh supported Be window transmitting 55 % at 1.5 keV and 85 % at 8 keV. The cooling of the detector is performed with the help of a small liquid Nitrogen reservoir connected to the detector cold finger by copper straps.
A second solid state detector is put just in front of the 2 pinhole to monitor the incident flux during the reflectivity measurements.

FIGURE 10 : X-RAY PENCIL BEAM CHANNEL GENERAL LAYOUT

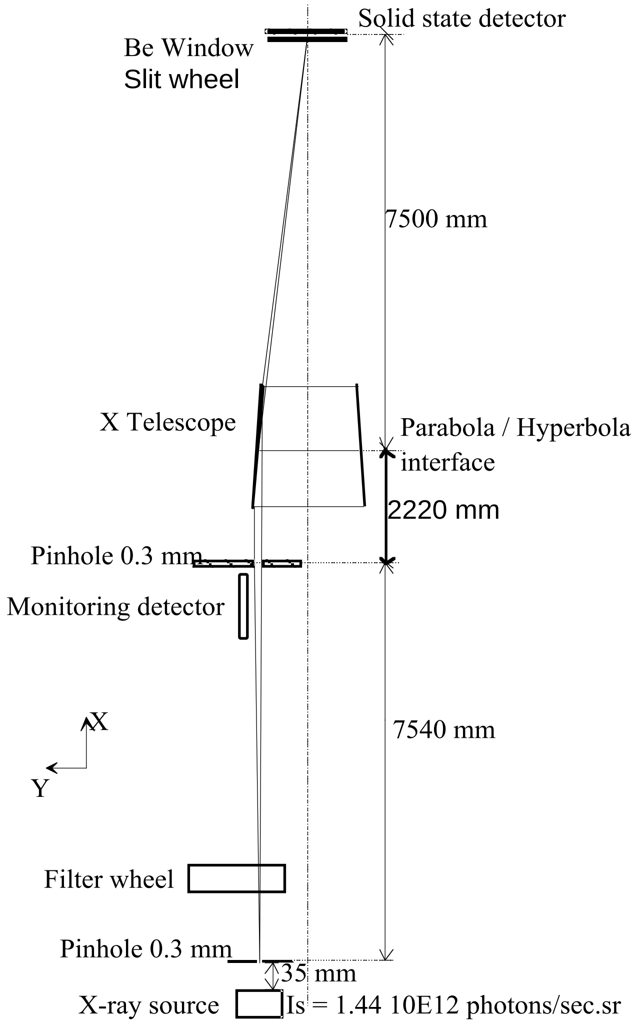

4.3. Reflectivity measurements at 1.5 and 8 keV

4.3.1. FM1 alignment procedure over X-ray pencil beam channel

To perform reflectivity measurement with the X ray pencil beam, the position inside the facility of each measured shell must be determined correctly. This is performed by scanning the FM1 MM in front of the pencil beam. The MM and the detector are translated along Y facility axis to scan all the FM1 shells once the detector position is optimised with respect to MS 58. The recorded signal during the scan gives a sinusoidal shape from which the position of the middle of each shell parabola is determined. A typical result is given in figure 11.

FIGURE 11 : TYPICAL DETECTOR RESPONSE DURING SCANNING OF THE SHELLS

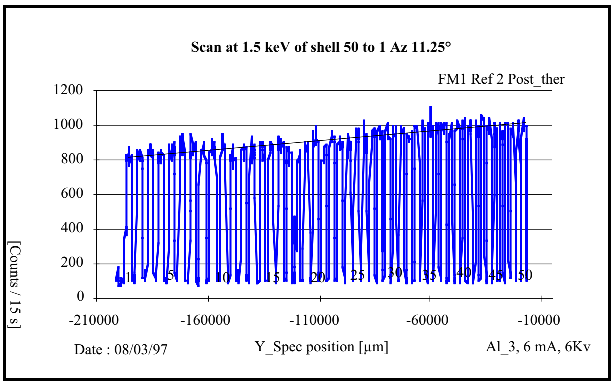

4.3.2. Reflectivity measurements

Reflectivity measurements are performed at the middle of the 10 smallest shells (58 to 49) for all the optical reference tests and for shells 40, 30, 20, 10, 1 (only for Post_thermal and Post_vibration) at 1.5 and 8 keV along two orthogonal azimuths. The reflectivity measurement is performed in a simple way. The direct beam signal is regularly recorded during 60 s. The reflected flux is integrated also during 60 s. During these acquisitions the source voltage and current are controlled before and after each measurement. No variation is observed on the anode voltage and a small drift 0.3 % over 12 hours for the current anode is observed.
The X monitoring records present variation of +/- 0.1 % to 0.2 %. Correction of the reflectivities by the monitoring data changes the reflectivity values by less than 0.5 % PTV.
The reflectivity is computed as the ratio of the counts in the region of interest of the reflected and incident beam.

4.4. Results

The results of the scans used for shell position determination for reflectivity measurements can also be used for metrological purpose. The results indicate that the shell position with respect to the nominal position is inside the measurement resolution that is 100 µm. These measurements show also that the position of the shells hasn't changed during the environmental test inside the measurement accuracy (100 µm).
As far as the reflectivities are concerned, it appears that at 8 keV the reflectivity is in average 6 to 7 % lower than the theoretical value, but that the differences between all the test are 1 % that is inside the measurement accuracy. At 1.5 keV a systematic decrease of 2 % appears after each environmental test. One explanation should be that the loss of reflectivity after each test could be due to accumulation of contamination inherent to the exposure of the test specimen. The performances at 8 keV are less affected by contamination than at 1.5 keV because of the penetrating power of the X rays. From the reflectivity data as well as from the shell position determination data, it is observed that the reflectivity on shell 54 is 13 % lower at 8 keV and 10 % at 1.5 keV than the theoretical value. This is correlated with the microroughness of the MS, which is high (7 Å) with respect to the average (< 4 Å) for this MS.

5. CONCLUSIONS

After these two months test of FM1 MM at CSL, it has been demonstrated and measured that there is no significative difference in terms of EEF before and after the environmental tests. The overall performance of the FM1 mirror modules after all these environmental tests is 15.5 arcsec for HEW, 62 arcsec for 90EW and 6.7 for FWHM, which are better than the required 16.5 arcsec for HEW and largely better with respect to the Qualification model tested one year before (19 arcsec for HEW). In terms of reflectivity, a systematic decrease appears at low energies (EUV effective area at 58.4 nm (21 eV) and reflectivity at 1.5 keV), that doesn't occur at higher energy (8 keV). A molecular contamination problem could be suspected, so that further investigations are running on this subject. Reflectivity measurements also show good correlation between poor microroughness and low reflectivity value. Hopefully, metrological data indicate that only a few shells have a micro roughness higher than 5 Å.

Acknowledgements

Many thanks go to our colleagues who worked during days and nights, week-ends included to collect all these precious data and information.
The vertical facility at CSL was funded by ESA XMM project under the contract number 9939/92/NL/PP.
The XMM FM1 mirrors were replicated and integrated by MEDIALARIO under ESA contract number 0545/93/NL/RE.

References

1. D. de Chambure, R. Lainé, K. van Katwijk, J. van Casteren & P. Glaude, " Producing the X-Ray Mirrors for ESA's XMM Spacecraft", ESA Bulletin 89, February 1997.
2. JP. Collette, Ph. Kletzkine, R. Lainé, Y. Stockman, JP. Tock, A. Vignelles, "Performances of XMM optics vertical test facility", SPIE 2808 p.350, Denver 1996.
3. J Ph. Tock, JP. Collette, I. Domken, Ph. Kletzkine, Y. Stockman, A. Vignelles, "A test facility for X-ray telescope", These proceedings.